Numerical model of turbulent pollutant transport in the atmospheric boundary layer

D.A. Belikov and A.V. Starchenko

Tomsk State University

Received February 7, 2007

An original model of turbulent pollutant transport is presented. Algebraic expressions for turbulent mass flows $<cu>$, $<cv>$, $<cw>$ in the form of simple gradient closure relations are derived within this model on the assumption of near-equilibrium turbulence. The model is tested with fundamental experimental data for various conditions of atmospheric stratification, dynamics of the atmospheric boundary layer, and turbulent dissipation of a pollutant from a surface source. The obtained relationships for turbulent mass flows are used in the model of pollutant transport taking into account the chemical transformations of transported substances in order to study the formation and dissipation of secondary pollutants in the air layer over a city and its suburbs.

Recently, works on the theory of atmospheric diffusion and pollutant dissipation based on the results of integration of the turbulent diffusion equation have gained a considerable development.[1–3] An advantage of this method is a possibility of taking into account the chemical reactions between pollutant components with the aid of atmospheric chemistry models.[4,5] This allows a detailed analysis of the anthropogenic impact on the environment on local scales. If computer systems with the parallel architecture significantly shortening the computational time for models of this level are used, the feasibility of obtaining a prompt and rather detailed prediction of evolution of an ecological situation on local and regional scales seems quite attractive.[6]

The pollutant concentration within the framework of the Euler continual approach is calculated by the model of turbulent diffusion including the transport equation[2–5]:

$$\frac{\partial C}{\partial t}+\frac{\partial UC}{\partial x}+\frac{\partial VC}{\partial y}+\frac{\partial W_cC}{\partial z}=$$

$$=-\frac{\partial}{\partial x}<cu>-\frac{\partial}{\partial y}<cv>-\frac{\partial}{\partial z}<cw_c>+S+R, \quad (1)$$

describing the advection, turbulent diffusion, pollution sources, and chemical reactions.[1] Here $C(t,x,y,z)$, $c(t,x,y,z)$ are the average and pulsation components of the pollutant concentration; (U,V), (u,v) are the average and pulsation horizontal components of the wind vector; W_c, w_c are the average and pulsation components of the pollutant velocity; S is the source term representing pollutant emissions into the atmosphere; R stands for chemical reactions with pollutant components in air; t is the time; (x,y,z) are coordinates.

Equation (1) is not closed, since, in addition to the sought concentration C, it includes other unknowns, namely, the correlations $<cu>$, $<cv>$, and $<cw_c>$ representing the turbulent diffusion of a pollutant and expressed through higher-order moments, which are very difficult to determine.[7] Nowadays the general understanding of this problem is achieved, and the approaches and methods (for example, the approach based on the Boussinesq gradient relationships[2,7]) are determined. In many simple cases, the use of these methods yields an acceptable result. However, for calculation of more complex processes, in particular, atmospheric ones, models based on equations for higher-order moments are required.

This paper proposes an original method for closure of the pollutant transport equation, whose essence consists in the following. The prognostic equations for determination of correlations $<cu_j>$ can be written in the form[9] (hereinafter we will use the index and component forms: $(u,v,w_c)=(u_1,u_2,u_3)=u_j$; $(x,y,z)=(x_1,x_2,x_3)$; $j=1,2,3$):

$$\frac{\partial<cu_j>}{\partial t}+U_i\frac{\partial<cu_j>}{\partial x_i}=-\left(<u_iu_j>\frac{\partial C}{\partial x_i}\right)-$$

$$-\left(<cu_i>\frac{\partial U_j}{\partial x_i}\right)+\frac{1}{\rho}\left\langle p\frac{\partial c}{\partial x_j}\right\rangle-\frac{1}{\rho}\frac{\partial<pc>}{\partial x_j}-\frac{\partial}{\partial x_i}<cu_iu_j>-$$

$$-g_j\frac{<c\theta>}{\Theta}+D\frac{\partial^2<cu_j>}{\partial x_i\partial x_i}-(D+\nu)\left\langle\frac{\partial c}{\partial x_i}\frac{\partial u_j}{\partial x_i}\right\rangle,$$

$$j=1,2,3; \quad (2)$$

where Θ, θ are the average and pulsation components of the potential temperature.

In the case of a near-equilibrium process, Equation (2) takes the form

$$-<u_ju_i>\frac{\partial C}{\partial x_i}+P_j+B_j+\Pi_j-\varepsilon_j=0,$$

$$j=1,2,3. \quad (3)$$

Here

$$P_j=-<cu_i>\frac{\partial U_j}{\partial x_i};\quad B_j=-g_j\frac{<c\theta>}{\Theta};$$

0235-6880/07/08 607-06 $02.00 © 2007 Institute of Atmospheric Optics

$$\Pi_j = \frac{1}{\rho}\left\langle p\frac{\partial c}{\partial x_j}\right\rangle;\ \ \varepsilon_j = (D+\nu)\left\langle \frac{\partial c}{\partial x_i}\frac{\partial u_j}{\partial x_i}\right\rangle.$$

According to Ref. 10, for $\Pi_j - \varepsilon_j$ we accept

$$\Pi_j - \varepsilon_j = -C_{1\theta}\frac{1}{\tau}<cu_j> - C_{2\theta}P_j - $$

$$- C_{3\theta}B_j - \delta_{j3}D_{1C}\frac{<cu_j>}{\tau}F,$$

$$j = 1, 2, 3; \qquad (4)$$

where F is the function determining the surface influence on the flow turbulent structure; $C_{1\theta} = 3.0$, $C_{2\theta} = 0.346$, $C_{3\theta} = 0.333$, and $D_{1C} = 0.806$ are empiric constants; $\tau = l/C_D\sqrt{k}$ is the time scale of turbulent pulsations; $\mathbf{g} = (g_j) = (0, 0, -g)$ is the free-fall acceleration vector; the last term in Eq. (4) takes into account the redistribution of turbulent mass flows near the surface; δ_{ji} is the Kronecker delta.

With allowance for Eqs. (4) and (3) take the form

$$-<u_iu_j>\frac{\partial C}{\partial x_i} + (1-C_{2\theta})P_j + (1-C_{3\theta})B_j -$$

$$-(C_{1\theta} + \delta_{j3}D_{1C}F)\frac{<cu_j>}{\tau} = 0,\ j = 1, 2, 3. \qquad (5)$$

Assuming that the temperature and wind velocity are functions only of time and the vertical coordinate and neglecting the vertical component of the wind velocity ($U_3 = 0$), we can solve Eq. (3) for $<cu_j>$:

at $j = 1$:

$$-<cu> = \frac{\tau}{C_{1\theta}}\left((1-C_{2\theta})<cw_c>\frac{\partial U}{\partial z} + <u_iu>\frac{\partial C}{\partial x_i}\right); \qquad (6)$$

at $j = 2$:

$$-<cv> = \frac{\tau}{C_{1\theta}}\left((1-C_{2\theta})<cw_c>\frac{\partial V}{\partial z} + <u_iv>\frac{\partial C}{\partial x_i}\right); \qquad (7)$$

at $j = 3$:

$$-<cw_c> = \frac{\tau}{C_{1\theta} + D_{1C}F}\left(-(1-C_{3\theta})\frac{g}{\Theta}<c\theta> + <u_iw_c>\frac{\partial C}{\partial x_i}\right). \qquad (8)$$

To find the unknown correlation between temperature and concentration pulsations $<c\theta>$ entering into Eq. (8), we derive the differential equation in the form[8,9,11]:

$$\frac{\partial <c\theta>}{\partial t} + U_i\frac{\partial}{\partial x_i}<c\theta> = -<cu_3>\frac{\partial \Theta}{\partial x_3} -$$

$$-<\theta u_i>\frac{\partial C}{\partial x_i} + \frac{\partial}{\partial x_i}\left(\alpha\frac{k}{\varepsilon}<u_iu_j>\frac{\partial <c\theta>}{\partial x_i}\right) - \frac{2}{\tau c_x}<c\theta>. \qquad (9)$$

It should be noted that in the case of slightly nonequilibrium turbulence, when the turbulence generation is nearly compensated by its dissipation, from Eq. (9) we can obtain

$$-<cw_c>\frac{\partial \Theta}{\partial z} - <\theta u_i>\frac{\partial C}{\partial x_i} - \frac{2}{\tau c_x}<c\theta> = 0,$$

or

$$<c\theta> = -\tau\frac{c_x}{2}\left(<cw_c>\frac{\partial \Theta}{\partial z} + <\theta u_i>\frac{\partial C}{\partial x_i}\right). \qquad (10)$$

With allowance for Eq. (10), Equation (8) acquires the form

$$-<cw_c> = \frac{\tau}{C_{1\theta} + D_{1\theta}F}\left(\tau(1-C_{3\theta})\frac{g}{\Theta}\frac{c_x}{2}<\theta u_i> + <u_iw_c>\right)\frac{\partial C}{\partial x_i}.$$

$$1 + \frac{\tau^2(1-C_{3\theta})}{(C_{1\theta} + D_{1\theta}F)}\frac{g}{\Theta}\frac{c_x}{2}\frac{\partial \Theta}{\partial z} \qquad (11)$$

Upon substitution of Eq. (11) into Eqs. (6) and (7), we obtain the equations for turbulent mass flows $<cu>$, $<cv>$, and $<cw_c>$, whose forms resemble the Boussinesq gradient closure equations: $<cu_i> = -K_{ij}\left(\partial C/\partial x_j\right)$. As they are substituted into the transport equation (1), there appear mixed derivatives, whose influence can be significant.[2]

Turbulent heat and momentum fluxes entering the obtained equations (6)–(8) [or (11)] are determined with the aid of algebraic relationships presented in Ref. 12.

It should be also noted that the correlations of concentration and temperature pulsations $<c\theta>$ can be calculated with the use of the transport equation (9).

Meteorological parameters and turbulent characteristics necessary for the transport model are determined using the nonstationary model in the approximation of the homogeneous atmospheric boundary layer (ABL).[13] In this case, the three-parameter "$k - l - <\theta^2>$" model of turbulence is applied. This model includes the prognostic equations for the energy and the scale of turbulence, as well as for the square temperature pulsations[13]:

$$\frac{\partial k}{\partial t} = -<uw>\frac{\partial U}{\partial z} - <vw>\frac{\partial V}{\partial z} +$$

$$+\frac{g}{\Theta}<w\theta> + \frac{\partial}{\partial z}\left(\sigma_e\sqrt{k}l\frac{\partial k}{\partial z}\right) - \frac{C_Dk^{\frac{3}{2}}}{l}; \qquad (12)$$

$$\frac{\partial l}{\partial t} = C_{l1}\left(-<uw>\frac{\partial U}{\partial z} - <vw>\frac{\partial V}{\partial z} + \frac{g}{\Theta}<w\theta>\right)\frac{l}{k} +$$

$$+\frac{\partial}{\partial z}\left(\sigma_e\sqrt{k}l\frac{\partial l}{\partial z}\right) + C_{l2}\sqrt{k}\left[1 - \left(\frac{l}{\kappa z}\right)^2\right], \qquad (13)$$

$$\frac{\partial <\theta^2>}{\partial t} = \frac{\partial}{\partial z}\left(C_\theta\sqrt{k}l<w>^2\frac{\partial <\theta^2>}{\partial z}\right) -$$

$$-2<w\theta>\frac{\partial \Theta}{\partial z} - 2\frac{<\theta^2>}{C_\theta\tau}. \qquad (14)$$

Here k is the kinetic energy of turbulence; l is the integral scale of turbulence; $\sigma_e = 0.54$, $C_{l1} = -0.12$, $C_{l2} = 0.2$, $C_D = 0.19$, and $C_\theta = 3.0$ are numerical coefficients; $\kappa = 0.41$. Turbulent momentum $<uw>$, $<vw>$ and heat $<w\theta>$ fluxes are determined with the aid of algebraic equations.[12]

The initial and boundary conditions, as well as the numerical method for solution of the differential equations of pollutant transport, are described in detail in Refs. 4 and 13.

An important parameter characterizing the state of the planetary boundary layer is thermal stratification (the character of the vertical distribution of the air temperature), which affects markedly the turbulent structure of the atmospheric boundary layer. Therefore, the model of homogeneous ABL was used for test calculations of turbulent stresses $\langle u^2\rangle$, $\langle v^2\rangle$, $\langle w^2\rangle$, temperature variance $\langle\theta^2\rangle$, turbulent heat $\langle w\theta\rangle$ and momentum $\langle uw\rangle$, $\langle vw\rangle$ fluxes for different regimes of ABL stratification.[11] The testing was carried out with the use of experimental data, results of other authors,[10,14–16] and calculations based on a simpler approach, namely, closure of the system of fluid dynamics equations in the form of the Boussinesq gradient relationships and turbulent diffusion relationships.[8,9]

The profiles of the normal turbulent stresses $\langle w^2\rangle$, $\langle u^2\rangle$, $\langle v^2\rangle$ (as functions of the vertical coordinate normalized to the height of the computational area H) calculated by the algebraic model and by the model with the Boussinesq relationships for the conditions of the boundary layer with neutral stratification and normalized to the square dynamic velocity v_* are shown in Figs. 1*a*–*c*.

The conditions of the ideal neutral boundary layer are observed very rarely in the atmosphere, and that is why there is not a complete data set for testing the model. However, it was indicated in Ref. 10 that the results of Refs. 17 and 18 (also shown in Fig. 1) are most suitable.

As was found in Ref. 10, the considering of the wall effects decreases the flux stresses and leads to the higher-quality prediction for the horizontal components of the stresses. That is why from here on the wall effects are taken into account in calculations by the algebraic model. In the case of the vertical normal stress $\langle w^2\rangle$, the contribution of the wall effects is not so unambiguous, but even in this case the calculated profile falls within the experimental data. Generally, the profiles of normal turbulent stresses obtained by the algebraic model are in a good agreement with the experimental findings and with the results of simulation.[10]

The profiles of the kinetic energy of turbulence are similar for the both versions and show somewhat underestimated values near the surface. Above the surface layer, these models, to the contrary, yield overestimated results compared to the model from Ref. 10 (Fig. 1*d*).

The experimental data and the calculated results for the kinetic energy of turbulence k were not initially presented in Ref. 10, but they were obtained as a result of the processing of values for the normal turbulent stresses through the use of the well-known relationship

$$k = \left(\langle u^2\rangle + \langle v^2\rangle + \langle w^2\rangle\right)/2.$$

The results of calculation of the stable boundary layer parameters in comparison with the experimental data[19,20] and the calculations[10] as a function of height normalized to the height of the surface layer h_s are shown in Fig. 2. In this case, the height of the surface layer is determined as a height, at which the tangential turbulent stress amounts to 5% of its value on the surface.

The profiles of the horizontal normal stress $\langle u^2\rangle$ (Fig. 2*a*) with allowance for the wall effects are in a good agreement with the measurements and calculations.[10] For $\langle w^2\rangle$ (Fig. 2*b*) we also obtained the decrease in the turbulent intensity with height.

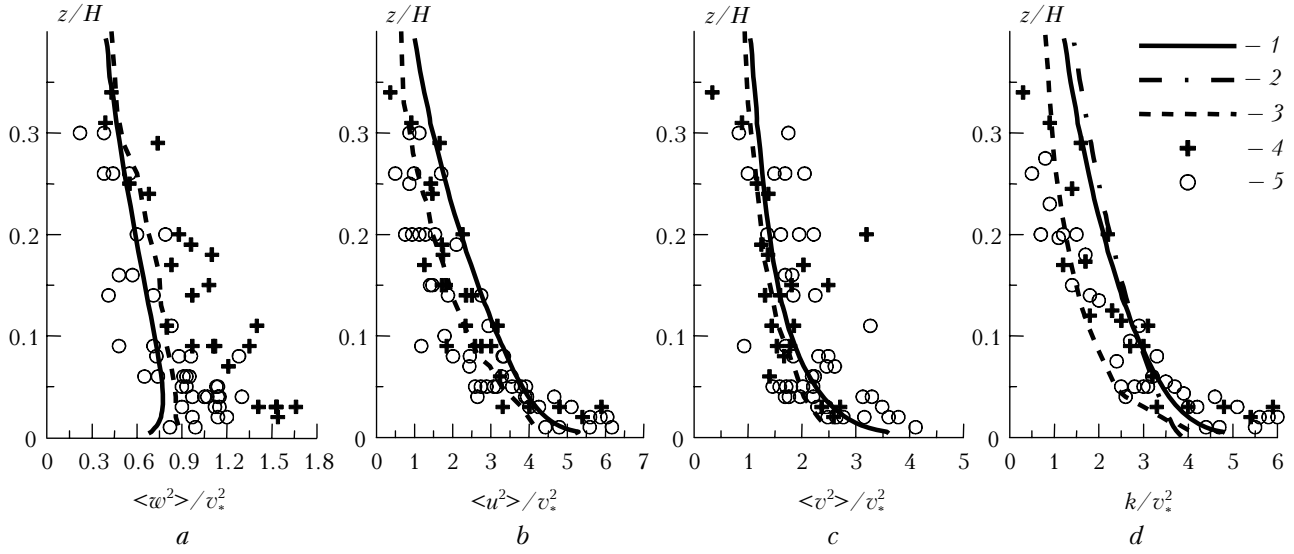

Fig. 1. Normal turbulent stresses $\langle w^2\rangle$, $\langle u^2\rangle$, $\langle v^2\rangle$ (*a*, *b*, *c*) and kinetic energy of turbulence (*d*) as functions of dimensionless height. Calculation by the proposed algebraic model (curve *1*), calculation by the model with the Boussinesq relationships (*2*), and calculation from Ref. 10 (*1*). Signs correspond to experimental data from Ref. 17 (*4*) and Ref. 18 (*5*).

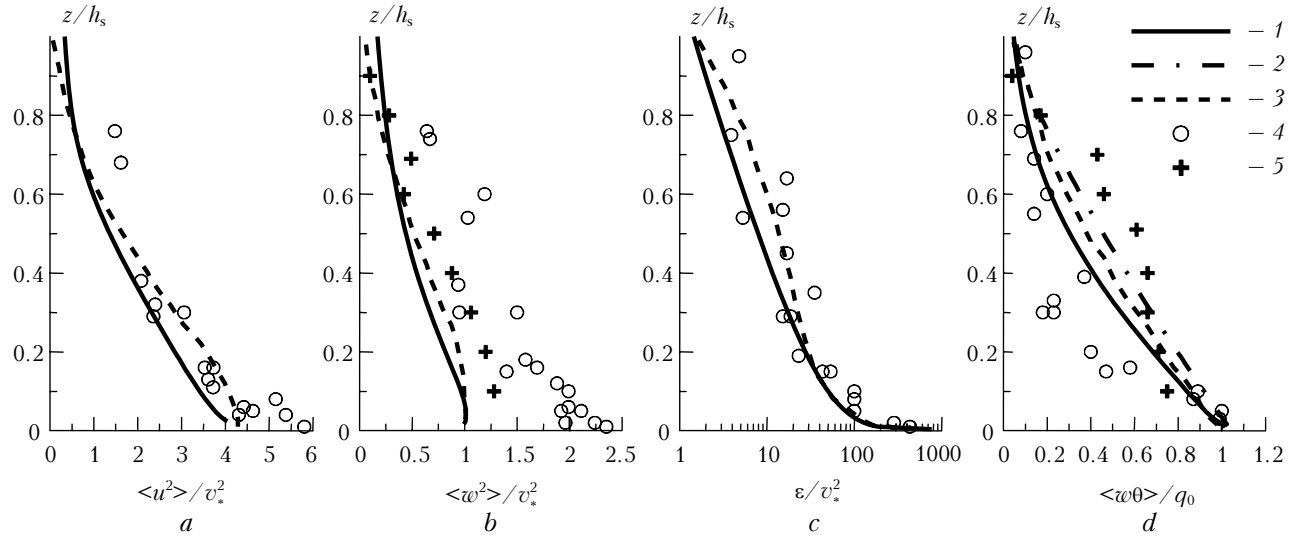

Fig. 2. Normal turbulent stresses $<u^2>$, $<w^2>$ (*a*, *b*), dissipation of the kinetic energy of turbulence (*c*), and the vertical heat flux (*d*) as functions of the dimensionless height. Designations are the same as in Fig. 1. Signs correspond to experimental data from Ref. 19 (*4*) and Ref. 20 (*5*).

The vertical distribution of dissipation of the kinetic energy of turbulence and the vertical heat flux for the considered case are also in a good agreement with the data of field observations (Figs. 2*c* and *d*).

The results of calculation for the convective boundary layer by the model presented in comparison with the experimental data[21] are shown in Fig. 3.

The profiles of turbulent parameters are plotted as functions of the height normalized to the height of the inversion layer z_i. In calculations, z_i is determined as a height, at which the horizontal heat flux $<\theta w>$ achieves the minimal negative value.[10]

The profile of the turbulent stresses $<w^2>$ normalized to the convective scale of velocity $w_* = \sqrt[3]{\beta g q_0 z_i}$ (Fig. 3*a*) achieves the maximal value $\cong 0.35$ at the height $z/z_i = 0.25$, as well as in both the theoretical [Ref. 15] and experimental [Ref. 22] works. Here q_0 is the heat flux on the surface; $\beta = 1/\Theta$ is the coefficient of volumetric expansion.

The dimensionless temperature variance $<\theta^2>/(q_0/w_*)^2$ decreases fast with the height from a value of about 40 near the surface to the minimum in the upper part of the boundary layer (Fig. 3*b*), and at high altitudes $<\theta^2>/(q_0/w_*)^2$ increases roughly up to 10–20 near the bottom boundary of the inversion layer[10,15] with the following decrease.

The adequate reconstruction of the dissipation of the turbulence kinetic energy by the model follows from the comparison of the calculated profile with the experimental and theoretical data[10,15] (Fig. 3*c*).

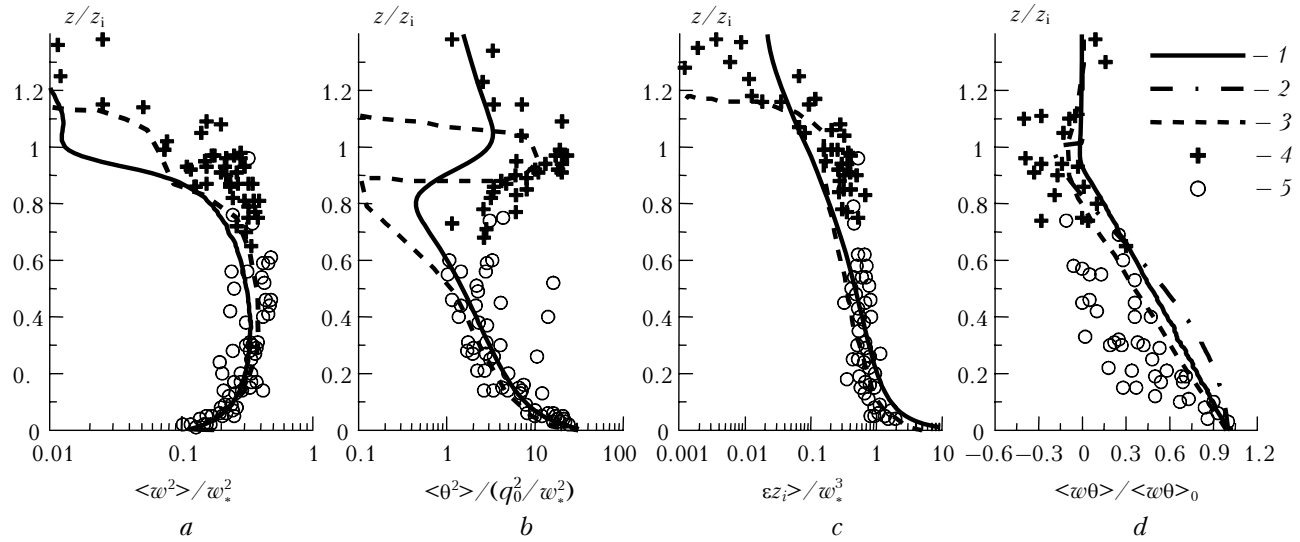

Fig. 3. Turbulent stress $<w^2>$ (*a*), variance of potential temperature $<\theta^2>$ (*b*), dissipation of the kinetic energy of turbulence (*c*), and vertical heat flux (*d*). Designations are the same as in Fig. 1. Signs correspond to experimental data from Ref. 19 (*4*) and Ref. 20 (*5*).

Figure 3*d* depicts the profile of the vertical turbulent heat flux $<\theta w>$ normalized to the heat flux on the surface. The shape of the profiles clearly indicates the influence of the entrainment processes between the heights of $0.6z_i$ and $1.0z_i$. Above the inversion layer, the flux quickly vanishes, which is in agreement with the data of the laboratory experiment[22] and the calculations of other authors.[10,15]

The test calculations of the nonstationary boundary layer dynamics over a homogeneous surface were preformed for the results of the Wangara Experiment, being one of the most successful and reliable field experiments on the study of the atmospheric boundary layer. The data of this experiment allow us to test the model for the conditions of nonstationary evolution of the atmospheric boundary layer over a homogeneous surface.[23]

Figure 4 compares the results of calculation by the model proposed and by the model using the Boussinesq gradient closure relationships and the turbulent diffusion coefficient with the data obtained in the Wangara Experiment.[23] It is clearly seen that the explicit anisotropic model better reconstructs the fine dynamic and thermal structure of ABL near the surface, while the use of the approach based on the concept of turbulent diffusion is inefficient in this case.

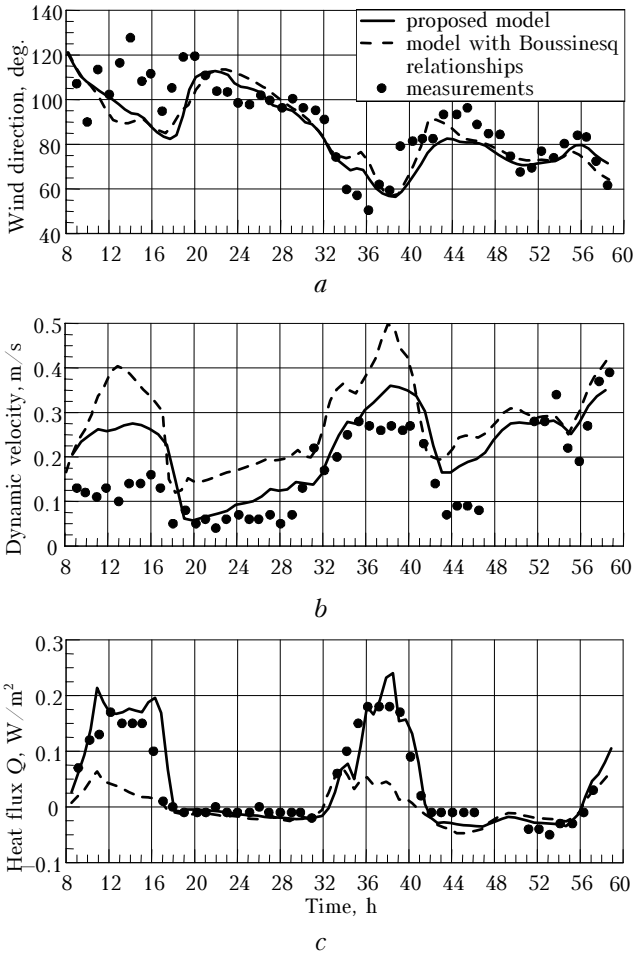

Fig. 4. Variations of wind velocity, dynamic velocity, and convective heat flux on the Earth's surface during the Wangara Experiment (33rd–34th days).

The further testing of the model was performed for the problem of pollutant transport and dissipation from an elevated continuous source in the convective boundary layer.

In developed convective ABL, a pollutant emitted by a surface continuous source moves in parallel with the surface, gradually lifting in the atmospheric mixing layer. A pollutant emitted by a source elevated above the surface is transported downward to the surface. This striking feature of the pollutant diffusion from an elevated source reflects the existence of the prevalent process of descent of a pollutant jet over the process of entrainment of the pollutant matter into smaller, quickly moving formations. This behavior is caused by the asymmetry of the probability density function of the vertical velocity of turbulent pulsations $<w^2>$, having the pronounced negative mode.[1,15]

The results of simulation of the pollutant dissipation from an elevated source with the height $z_s = 0.24z_i$ are shown in Fig. 5 in comparison with the data of the field experiment.[24] Here $C_y^* = C_y(x, z)z_iU_s/Q_i$ is the dimensionless pollutant concentration; z_i is the height of the inversion layer; the axis x^* is equivalent to the dimensionless distance in the downstream direction along the flow from the source $x^* = xw_*/U_sz_i$; $z^* = z/z_i$ is the dimensionless vertical coordinate; U_s is the wind velocity at the height of the source; $C_y(x, y)$ is the pollutant concentration averaged over the vertical coordinate Oy normal to the direction of the wind vector; Q_i is the source emission rate. The results of calculations by the model are in a good agreement with the experimental results. First, the plume from the elevated source sinks and touches the Earth's surface between $0.5x^*$ and $1.0x^*$, and then it begins to rise.

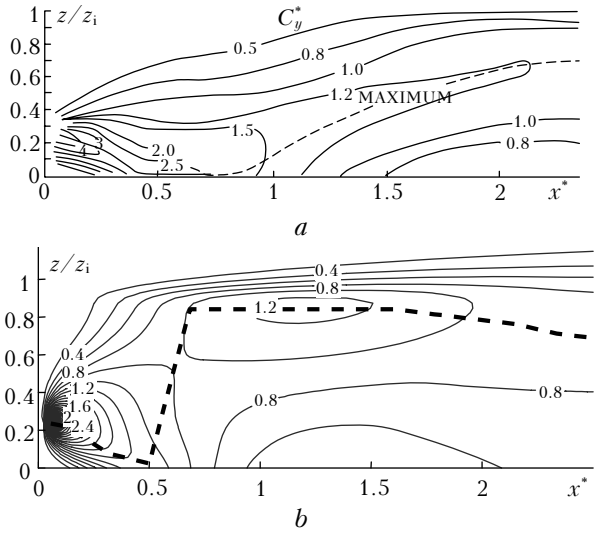

Fig. 5. Isolines of the dimensionless pollutant concentration C_y^* in the plane OX^*z^*; source height $z_s = 0.24z_i$; experimental results[24] (*a*) and result of simulation with the use of algebraic relationships (*b*).

The conditions used in the calculations and the data for comparisons are borrowed from Ref. 15.

The dissipation of a pollutant from a near-surface source with the height $z_s = 0.067 z_i$ is shown in Fig. 6.

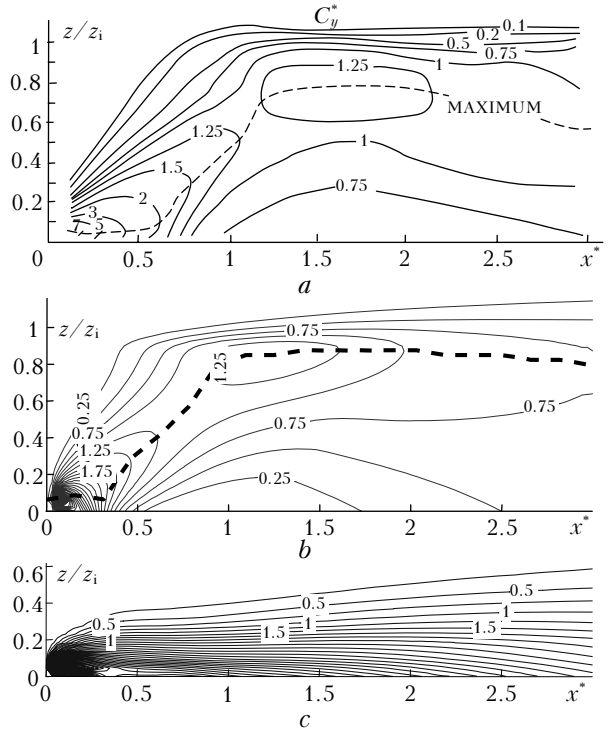

Fig. 6. Ioslines of dimensionless concentration of a pollutant from a source with the height $z_s = 0.067 z_i$; experimental results (*a*),[24] results of simulation by the model proposed (*b*), and result of simulation with the use of the Boussinesq relationships (*c*).

The results of calculations by the model proposed are in a good agreement with the experimental results, while the locally isotropic model using the Boussinesq closure relationships (Fig. 6*c*) under these conditions fails to reconstruct the fine structure of the turbulent dissipation of a pollutant.

The results of testing of the proposed numerical model based on the original scheme of closure of the transport equation and on the algebraic relationships for turbulent momentum, heat, and mass fluxes have demonstrated a good agreement with the results of field observations under different conditions of ABL temperature stratification and the Wangara Experiment. For the cases of neutral and stable stratification, the approach proposed is comparable with the Boussinesq gradient relationships. However, in the case of the convective boundary layer and nonstationary changes in ABL, for example, during a day, the Boussinesq approach appears to be inefficient (see Fig. 4). When the pollutant dissipation from a continuous source in convective ABL is considered, the Boussinesq approach turns out to be inapplicable (see Fig. 6).

The relationships proposed for closure of the transport equation added by algebraic equations are used in the model of pollutant transport[4,11] and can be applied to a wide range of similar transport problems.

Since the application of high-accuracy models of pollutant transport imposes additional requirements on the quality of modeling the turbulent transport in the surface atmospheric layer, the use of algebraic models is preferable.

Acknowledgements

This work was supported in part by the Russian Foundation for Basic Research (Grants Nos. 04–07–90219, 05–98010r-Ob, and 07–05–01126).

References

1. F.T.M. Nieustadt and H. Van Dop, eds., *Atmospheric Turbulence and Air Pollution Modeling* (D. Reidel, Dordrecht–Boston–London, 1982).
2. M.E. Berlyand, *Prediction and Regulation of Atmospheric Pollution* (Gidrometeoizdat, Leningrad, 1985), 168 pp.
3. V.V. Penenko, *Methods for Numerical Simulation of Atmospheric Processes* (Gidrometeoizdat, Leningrad, 1981), 351 pp.
4. D.A. Belikov and A.V. Starchenko, Atmos. Oceanic Opt. **18**, Nos. 5–6, 391–398 (2005).
5. P.J. Hurley, CSIRO Atmos. Res. Tech. Paper, No 55, 37 (2002).
6. D. Dabdub and J.H. Seinfeld, Parallel Computing **22**, 111–130 (1996).
7. A.F. Kurbatskii, *Lections on Turbulence*, in two volumes (Novosibirsk State University Press, Novosibirsk, 2000).
8. L.G. Loitsyanskii, *Fluid and Gas Mechanics*. Students' Book (Drofa, Moscow, 2003), 840 pp.
9. W. Kollmann, ed., *Prediction Methods for Turbulent Flows* (Hemisphere Publishing Corporation, Washington, D.C., 1979).
10. A. Andren, J. Appl. Meteorol. **29**, 224–239 (1990).
11. D.A. Belikov, "Parallel realization of the mathematical model of atmospheric diffusion for investigation of the distribution of primary and secondary air pollutants over an urban territory," Cand. Phys.-Math. Sci. Dissert., Tomsk State University, Tomsk (2006), 177 pp.
12. A.V. Starchenko, in: *Proc. of Int. Conf. ENVIROMIS-2000* (Tomsk, 2000), pp. 77–82.
13. A.V. Starchenko and D.A. Belikov, Atmos. Oceanic Opt. **16**, No. 7, 657–665 (2003).
14. B.B. Ilyushin and A.F. Kurbatskii, Izv. Ros. Akad. Nauk. Fiz. Atmos. Okeana **30**, No. 5, 615–622 (1994).
15. B.B. Ilyushin and A.F. Kurbatskii, Izv. Ros. Akad. Nauk. Fiz. Atmos. Okeana **32**, No. 3, 307–321 (1996).
16. P. Duynkerke, J. Atmos. Sci. **45**, 865–879 (1988).
17. R. Brost and H. Lenschow, J. Atmos. Sci. **39**, 818–836 (1982).
18. A.L.M. Grant, Quart. J. Roy. Meteorol. Soc. **112**, 825–841 (1986).
19. S.J. Caughey, J.C. Wyngaard, and J.C. Kaimal, J. Atmos. Sci. **36**, 1041–1052 (1979).
20. F.T.M. Nieustadt, J. Atmos. Sci. **41**, 2202–2216 (1984).
21. S.J. Caughey and S.G. Palmer, Quart. J. Roy. Meteorol. Soc. **105**, 811–827 (1979).
22. G.E. Willis and J.W. Deardorff, J. Atmos. Sci. **31**, 1297–1307 (1974).
23. T. Yamada and G. Mellor, J. Atmos. Sci. **32**, 2309–2329 (1975).
24. G.E. Willis and J.W. Deardorff, Atmos. Environ. **12**, 1305–1311 (1978).